Journal of Tropical Forest Science 37(Special Issue): 48–73 (2025)
https://doi.org/10.26525/jtfs2025.37S.SI.48
ISSN: 0128-1283, eISSN: 2521-984

EXPLORING POTENTIAL PHYTOCHEMICAL INHIBITORS OF SARS-COV-2 MAIN PROTEASE (3CL^{PRO}) FROM MALAYSIAN PLANTS: A MOLECULAR DOCKING STUDY

Maram B. Alhawarri[1], *, Dania F. Alsaffar[2] & Mohammad G. Al-Thiabat[3]

[1]Department of Pharmacy, Faculty of Pharmacy, Jadara University, P.O. Box 733, Irbid 21110, Jordan
[2]College of Dentistry, Ibn Sina University of Medical and Pharmaceutical Sciences, Baghdad, Iraq
[3]Department of Pharmacy, Faculty of Pharmacy, Jerash University, P.O. Box 311, Jerash 26150, Jordan

**m.hawarri@jadara.edu.jo*

Submitted May 2024; accepted December 2024

The COVID-19 pandemic, caused by SARS-CoV-2, has created a global health crisis. The 3-chymotrypsin-like protease (3CLpro), essential for viral replication, is a key therapeutic target. This study aimed to screen 42 Malaysian medicinal plants, containing over 250 bioactive compounds, for their inhibitory potential against SARS-CoV-2 3CLpro using in silico methods. Among these, 11 compounds—lensoside Aβ (*Lens culinaris*), persicoside D (*Allium ampeloprasum*), 2",2"'-di-O-α-rhamnopyranosyl vicenin II (*Beta vulgaris*), quercetin-7-O-rutinoside (*Asplenium nidus*), officinoterpenoside E (*Solanum melongena*), basilmoside (*Ocimum basilicum*), apigenin 7-O-β-D-apiofuranosyl glucopyranoside (*Apium graveolens*), racemosol and stigmasta-7,22-dien-3β,4β–diol (*Lagenaria siceraria*), α-hederine (*Nigella sativa*), and inermidioic acid (*Lawsonia inermis*)—demonstrated stronger binding affinities than the reference inhibitor N3. Molecular interaction analysis showed these compounds formed stable interactions with key 3CLpro residues, indicating their potential as lead molecules for drug development. Additionally, the corresponding plants could serve as natural sources of alternative COVID-19 therapies. These findings warrant further experimental validation to explore their therapeutic potential against SARS-CoV-2.

Keywords: COVID-19, 3CL^{pro}, molecular docking, medicinal plants, phytochemicals

INTRODUCTION

In December 2019, the first case of coronavirus disease 2019 (COVID-19) was reported in Wuhan, China (Afshar et al. 2020, Fani et al. 2020). COVID-19, caused by SARS-CoV-2, can range from mild to fatal, with severity influenced by patient factors such as age, immune system status, and pre-existing conditions (Brodin 2021). The virus has a significant mortality rate, particularly in older adults with chronic health conditions (Ebinger et al. 2020, Guo et al. 2020, Long et al. 2020). Human coronaviruses (HCoVs), responsible for upper respiratory tract infections, include both low and high pathogenic types (Coerdt & Khachemoune 2021, Kesheh et al. 2022, Sealy & Hurwitz 2021). High pathogenic HCoVs, such as SARS-CoV and MERS-CoV, are linked to more severe respiratory illnesses (Mostafa et al. 2020, Paules et al. 2020, Zhu et al. 2020). SARS-CoV-2 shares a high genetic similarity with SARS-CoV, both belonging to the beta-coronavirus subgroup (Chathappady House et al. 2021, Peddu et al. 2020, Shang et al. 2021). Researchers have relied on previous SARS studies to understand the mechanisms of SARS-CoV-2 (Blankenship et al. 2024, Chen et al. 2024, Li et al. 2022, Qiao et al. 2021).

The SARS-CoV-2 spike glycoprotein binds to the angiotensin-converting enzyme 2 (ACE2), facilitating viral entry into host cells (Monti et al. 2024, Peng et al. 2024). Following ACE2 binding, the viral RNA genome is released and processed into polyproteins, which are cleaved by proteases such as 3CL^{pro} (El Khoury et al. 2024, Schwartz et al. 2024, Yang et al. 2024). Given its critical role in viral replication and the absence of a human counterpart, 3CLpro has become a target for antiviral drug development (Cannalire et al. 2020, de Vries et al. 2020, de Vries et al. 2021). While several drugs and vaccines have been approved for COVID-19 (Kalinke et al. 2022, Mahrokhian et al. 2024, Pai et al. 2021), the search for additional therapeutic agents continues (Marrazza

et al. 2024). Protease inhibitors, including Lopinavir/Ritonavir, have shown potential for treating COVID-19, drawing on their previous success against SARS and MERS (Chaudhuri et al. 2018, De Clercq & Li 2016, Srivastava & Singh 2021).

Natural products have been used to treat various viral infections, and some have demonstrated the ability to inhibit viral replication (Boozari & Hosseinzadeh 2021, Li et al. 2024, Musarra-Pizzo et al. 2021). According to reports in the Annual Reports in Medicinal Chemistry, between 1948 and 1995, seven out of ten antivirals approved by the FDA were either naturally derived or based on natural models (Lowe et al. 2021, Woster 2009). Podofilox (Condylox) is an example of a naturally occurring antiviral agent extracted from the podophyllum resin of the May apple (*North American Podophyllum peltatum* or *Indian Podophyllum emodi*) (De Clercq & Li 2016). Furthermore, between 1948 and 2017, 37.5% of antiviral drugs approved by the FDA were primarily polymerase-targeting agents, while 23.6% of them were protease-targeting antiviral agents (Chaudhuri et al. 2018).

Computational methods, particularly molecular docking, have become essential tools in drug discovery (Moshawih et al. 2023, Tripathi et al. 2021, Wu et al. 2020). Docking simulations allow the prediction of ligand binding conformations based on free binding energy calculations, identifying compounds with the strongest interactions with a target protein (Alhawarri et al. 2024b, Alhawarri & Olimat 2024, De Ruyck et al. 2016, Ferreira et al. 2015, Kaur et al. 2019). Over the past decade, docking tools such as AutoDock 1.5.6 has been widely used for this purpose (Alidmat et al. 2022b, Hazarika & Jha 2020, Yunos et al. 2023, Yunos et al. 2024). In this study, a panel of known chemical constituents isolated from Malaysian medicinal plants were screened in silico against the $3CL^{pro}$ of SARS-CoV-2. The aim was to identify potential antiviral drug candidates by comparing them to the Michael acceptor inhibitor (N3), a potent irreversible inhibitor of $3CL^{pro}$. These identified compounds may serve as candidates for further therapeutic evaluation and drug development.

MATERIALS AND METHODS

Protein preparation

The human crystal structure for COVID-19 main protease ($3CL^{pro}$) was downloaded from the Protein Data Bank database (PDB ID: 6LU7) (Jin et al. 2020). To ensure the precision of the structural analysis, all water residues (including those present at the active binding site) and heteroatom molecules were eliminated using the Biovia Discovery Studio Visualizer 16.1 (San Diego, CA, USA) (Biovia 2017), a crucial step for minimising inaccuracies (Alhawarri et al. 2023b, Alhawarri 2024, Alhawarri et al. 2024b, Alhawarri & Olimat 2024, Alidmat et al. 2024, Al-Thiabat et al. 2021a, Ibrahim et al. 2024, Yunos et al. 2023, Yunos et al. 2024). The enzyme was then prepared for molecular docking through the PDB2PQR web service (https://pdb2pqr.poissonboltzmann.org/pdb2pqr), accessed on March 17th, 2024. This service facilitated the reconstruction of missing atoms, and the assignment of atomic charges and radii according to the SWANSON force field (employing AMBER ff99 charges with optimised radii) (Alhawarri et al. 2023b, Alhawarri et al. 2024a, Al-Thiabat et al. 2021a, Amir Rawa et al. 2022, Dolinsky et al. 2007, Larue et al. 2023, Yunos et al. 2024). The protonation states of ionizable groups were established using the empirical pKa predictor PROPKA3, set at pH 7.4, to mirror physiological conditions (Alhawarri et al. 2023b, Amir Rawa et al. 2022, Larue et al. 2022, Olsson et al. 2011). Following protonation, the enzyme underwent a refinement process via the MolProbity web service (http://molprobity.biochem.duke.edu/) on March 17th, 2024, to correct atomic contacts and append missing hydrogen atoms (Williams et al. 2018), ensuring the integrity and accuracy of the structural analysis (Alhawarri et al. 2023b, Al-Thiabat et al. 2021a).

Active site prediction

All possible binding sites of the $3CL^{pro}$ (6LU7) were searched by active analysis of the PrankWeb server (Http:/prankweb.cz/) (Jendele et al. 2019). Four possible binding sites have been identified in 6LU7. The largest site with the highest pocket score has been selected. Furthermore, the selected binding site was also

supported by the fact that the Michael inhibitor (N3) was bonded to this site. The selected center pocket score of 6LU7 was -10.2439 (X), 17.966 (Y), and 66.5084 (Z).

Ligands preparation

Based on clinical studies and literature reviews, 42 of Malaysian medicinal plants which possess antiviral activity were selected to study the potential binding affinity with the specific binding sites of $3CL^{pro}$ COVID-19. The selected medicinal plants were reported to have antiviral activity including; *Euphorbia neriifolia* (Chang et al. 2012), *Euphorbia hirta* (Kumar et al. 2010), *Andrographis paniculata* (Tang et al. 2012, Wiart et al. 2005), *Momordica charanthia* (Bourinbaiar & Lee-Huang 1996, Tang et al. 2012), *Leucaena leucocephala* (Ono et al. 2003), *Psidium guajava* (Sriwilaijaroen et al. 2012), *Morinda elliptica* (Hamidi et al. 1996), *Piper sarmentosum* (Hussain et al. 2012), *Trichosnathes kirilowii* (Chen et al. 2006), *Morinda citrifolia* (Ratnoglik et al. 2014), *Houttuynia cordata* (Choi et al. 2009, Chiow et al. 2016, Hayashi et al. 1995), *Lobelia chinensis* (Kuo et al. 2011), *Elephantopus scaber* (Geng et al. 2011), *Calotropis gigantean* (Parhira et al. 2014), *Melastoma malabathricum* (Joffry et al. 2012), *Asplenium nidus* (Tahir et al. 2014), *Eleusine indica* (Tahir et al. 2014, Iberahim et al. 2015), *Phaleria macrocarpa* (Tahir et al. 2014), *Nigella sativa* L. (Ulasli et al. 2014), *Camellia sinensis* (Mahmood et al. 2016), *Durio zibenthinus* (Nikomtat et al. 2017), *Cinnamomum zeylanicum Blume* (Fabros Jr et al. 2018), *Cocos nucifera* (Esquenazi et al. 2002), *Cymbopogon schoenanthus* (Khalil et al. 2017), *Citrullus lanatus* (Omigie & Agoreyo 2014), *Phoenix dactylifera* (Jassim & Naji 2010), *Allium cepa* (Harazem et al. 2019, Romeilah et al. 2010), *Solanum melongena* (Di Sotto et al. 2018), *Allium sativum* (Romeilah et al. 2010), *Lawsonia inermis* (Mouhajir et al. 2001), Trigonella foenum-graecum (Hussein et al. 2000), *Ocimum basilicum* (Chiang et al. 2005), *Zingiber officinalle* (San Chang et al. 2013), *Senna alexandrina* (Ikram et al. 2023), *Beta vulgaris* (Betancur-Galvis et al. 1999), *Hordeum vulgare* (Sinha et al. 2012), *Musa acuminata* (de Camargo et al. 2020), *Lens culinaris* (Chatzivassiliou et al. 2016, Wang et al. 2021), *Apium graveolens* (Choochote et al. 2004), *Allium porrum* (Chen et al. 2011, Keyaerts et al. 2007), *Curcuma longa* (Ichsyani et al. 2017), *Lagenaria siceraria* (Kumar et al. 2015). Several active compounds of the medicinal plants have been obtained via Dr Duke's Phytochemical and Ethnobotanical Databases (https:/phytochem.nal.usda.gov/phytochem /search/list) (Lans & van Asseldonk 2020). Then, they were subjected to energy minimisation (MM2 force field) using PerkinElmer Chem3D 17.1 (Alhawarri et al. 2023b, Alhawarri 2024, Alhawarri & Olimat 2024, Alhawarri et al. 2024b, Alidmat et al. 2022b, Alidmat et al. 2024, Al-Thiabat et al. 2021a, Ibrahim et al. 2024, Yunos et al. 2023, Yunos et al. 2024). All downloaded compounds after the minimisation step were saved in PDB format.

Molecular docking

A summary workflow for the molecular docking simulation is presented in Figure 1. This part was achieved by using AutoDock 4.2 software (Norgan et al. 2011), where all rotatable bonds of the compounds were set randomized as completely flexible during the simulation process.

Polar hydrogens and Kollman charges were added to 3CLpro and saved as PDBQT. Gasteiger charges for the selected compounds were computed and also saved in PDBQT format. The grid box size was set to 40*40*40 for the prospective binding sites, coordinates (as X, Y, Z respectively) of the 1st binding site was -10.2439, 17.966, and 66.5084. A maximum number of 100 runs were chosen for each independent Lamarckian genetic algorithm (Fuhrmann et al. 2010). While remaining parameters were kept as default. AutoDock 4.2 was used to simulate the docking process. The 2D and 3D potential were visualised and analysed by the Biovia Discovery Studio Visualizer 16.1, to be able easily observed the hydrogen bonds, and the hydrophobic interactions.

RESULTS

Molecular docking has become an indispensable tool in the field of drug discovery, particularly for its role in expediting the identification of potential therapeutic agents (Ferreira et al. 2015, Gschwend et al. 1996). This computational method allows for the prediction of optimal binding conformations between small molecules

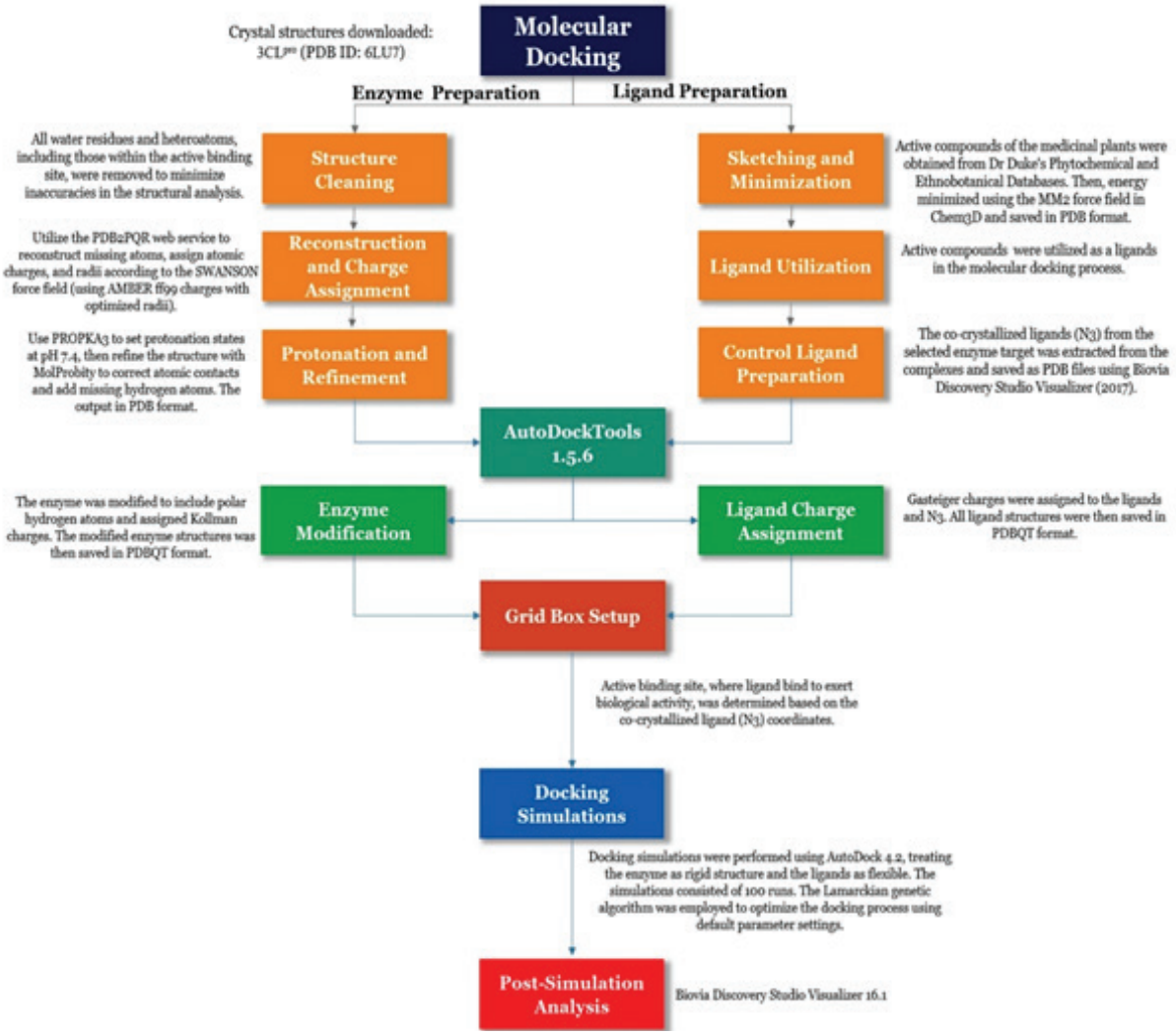

Figure 1 Summary of the molecular docking simulation workflow

and target proteins by evaluating the free binding energy of ligand-receptor complexes (Ferreira et al. 2015, Gschwend et al. 1996). Such simulations enable the efficient screening of large compound libraries, significantly reducing the time and resources required for the initial stages of drug development (Zhang et al. 2022). Molecular docking provides critical insights into the molecular interactions that govern ligand binding, including hydrogen bonding, van der Waals forces, hydrophobic interactions, and π-π stacking (Luo et al. 2019). These interactions are key determinants of a compound's binding affinity and inhibitory potential. In the context of SARS-CoV-2, the main protease ($3CL^{pro}$) has been widely recognized as a promising target due to its essential role in viral replication and the absence of a human counterpart (Cannalire et al. 2020, Liu et al. 2022).

$3CL^{pro}$ is a cysteine protease that plays a critical role in the viral life cycle by processing the viral polyproteins required for replication and transcription (Konwar & Sarma 2021, Yan & Wu 2021). As a vital enzyme, $3CL^{pro}$ has emerged as a prominent target for antiviral drug development (Konwar & Sarma 2021, Yan & Wu 2021). Structurally, $3CL^{pro}$ consists of three domains, with the active site located between domains I and II (Ferreira et al. 2022, Novak & Potemkin 2022). The catalytic dyad within the active site is composed of two key residues: HIS41 and CYS145 (Ferreira et al. 2021, Shalayel et al. 2020, Zanetti-Polzi et al. 2021). These residues are crucial for the protease's enzymatic activity,

facilitating the cleavage of peptide bonds in the viral polyproteins (Ferreira et al. 2021Shalayel et al. 2020, Zanetti-Polzi et al. 2021). In addition to the catalytic dyad, other residues such as GLU166, GLN189, and HIS163 contribute to substrate recognition and stabilization of the ligand within the binding pocket (Akbulut 2022, Weng et al. 2021). The hydrophobic pocket formed by residues like MET49, LEU141, and HIS164 further enhances ligand binding by promoting hydrophobic interactions (Jiang et al. 2024, Jin et al. 2020, Stoddard et al. 2020). Understanding the nature of these residues and their interactions with inhibitors is essential for designing potent 3CL^{pro} inhibitors that can block viral replication (Gupta et al. 2021). Molecular docking studies focusing on these residues provide valuable insights into the binding mechanisms of potential therapeutic compounds, helping to identify inhibitors with strong and specific interactions within the active site.

In this study, 42 medicinal plants previously known for their bioactive efficacy against various types of viruses were selected for further investigation. More than 290 bioactive compounds were initially identified from these plants, but due to overlapping compounds found across different plants, approximately 250 unique compounds were ultimately evaluated using an in silico approach (see Table S1). The aim was to explore their binding affinities to interact with 3CL^{pro} active site. The molecular docking protocol was initially validated by re-docking the original co-crystallized ligand (N3) within the active binding site of 3CLpro, using the crystal structure with PDB ID: 6LU7 (Figure S1).

The co-crystallised ligand Michael acceptor inhibitor (N3) was used as a reference to validate the molecular docking protocol. In its original pose (Figure 2), N3 demonstrated key interactions within the active site of 3CL^{pro}, forming hydrogen bonds with residues ASN142 (2.89 Å), GLY143 (2.62 Å), and GLN189 (3.04 Å). Additionally, hydrophobic interactions were observed with residues LEU27, HIS41, CYS145, HIS163, and MET165, further stabilising the ligand within the binding pocket. The re-docked pose of N3 (Figure S1) closely replicated these interactions, with only slight variations in the hydrogen bond distances, confirming

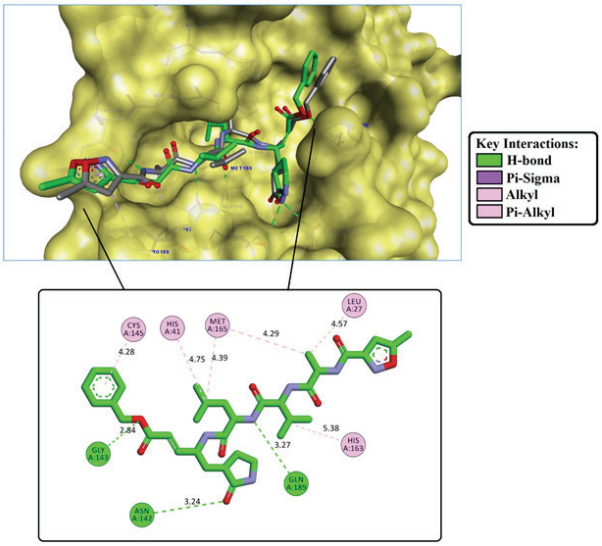

Figure SI Superimposition and 2D interaction analysis of the co-crystallized ligand, Michael acceptor inhibitor N3 (gray C, red O, and blue N), and the re-docked N3 (green C, red O, and blue N). The crystal structure of SARS-CoV-2 3CL^{pro} in complex with Michael acceptor inhibitor N3 (PDB ID: 6LU7) (RMSD = 1.22 Å)

the reliability of the docking protocol. The root-mean-square deviation (RMSD) of 1.22 Å between the original and re-docked poses falls well within the acceptable threshold of 2 Å (Alhawarri et al. 2023a, Alhawarri 2024, Alhawarri et al. 2024b, Alhawarri & Olimat 2024, Alidmat et al. 2022a, Alidmat et al. 2024, Al-Thiabat et al. 2021a, Amir Rawa et al. 2022, Ibrahim et al. 2024, Larue et al. 2023, Yunos et al. 2023, Yunos et al. 2024), indicating that the docking process accurately reproduced the binding conformation of N3. The free binding energy of N3 (redocked pose) was calculated to be -5.49 kcal/mol, which served as a control for evaluating the binding affinities of other compounds.

Table 1 Molecular docking scores

Compounds	Free binding energy (kcal/mol)	Molecular interactions analysis within the 3CLpro active binding site			
		H-bond	Distance (Å)	Pi-Sigma / Pi-Anion	Hydrophobic interaction
Lensoside Aβ	-9.88	THR26	3.12	GLU166 (Pi-Anion)	
		ASN119	4.40		
		PHE140	2.95 and 3.40		
		CYS145	3.01		
		HIS164	3.01 and 3.31		
		GLU166	2.65, 2.85, and 2.91		
		GLN189	2.96		
Persicoside D	-9.27	THR24	2.67		LEU27, HIS41, CYS145, HIS163 and HIS172
		ASN119	2.44, 2.97, and 3.03		
		ASN142	2.69		
2”,2”’-di-O–α-rhamnopyranosyl-vicenin II	-9.22	THR26	3.04	GLN189 (Pi-Sigma)	HIS41 and MET165
		SER46	2.68 and 2.99		
		PHE140	3.14		
		GLY143	2.78 and 3.2		
		CYS145	3.29		
		HIS163	2.97		
		HIS164	3.27		
		GLN189	2.62		
		THR190	2.69		
Quercetin-7-O-rutinoside	-8.97	THR24	2.81 and 3.29	THR25 (Pi- Sigma)	HIS163 and HIS172
		THR25	2.95		
		THR26	2.74 and 3.23		
		HIS41	2.82		
		THR45	2.62 and 2.91		
		SER46	3.15		
		LEU141	2.71		
		GLY143	3.13 and 3.24		
		SER144	2.52 and 3.38		
		CYS145	3.14, 3.04, and 3.66		
		HIS163	3.00		
		GLN189	3.40		

continued

Table 1 Continued

Compounds	Free binding energy (kcal/mol)	Molecular interactions analysis within the 3CLpro active binding site			
		H-bond	Distance (Å)	Pi-Sigma / Pi-Anion	Hydrophobic interaction
Officinoterpenoside E	-8.91	THR24 PHE140 GLY143 CYS145 HIS163	2.89 2.74 and 3.04 2.68 3.06 and 3.75 2.81 and 3.09	HIS41 (Pi- Sigma)	HIS41, MET49, and MET165
Basilmoside 24-ethyl-25-methylcholesta-5,22-dien-3-β-O-D-glucoside	-8.87	ARG188 THR190 GLN192	2.59 2.57, 2.69, and 3.39 3.14		HIS41, MET49, and CYS145
Apigenin 7-O-β-D-apiofuranosyl(1→2)-β-D-glucopyranoside	-8.76	THR26 THR45 SER46 LEU141 CYS145 HIS164 GLU166	2.94 and 3.21 2.49 3.11 3.01 3.06 and 3.40 3.20 2.70, 2.77, and 3.92		
Racemosol	-8.66	THR26	2.59	HIS41 (Pi- Sigma)	LEU27, HIS41, MET49, CYS145, HIS164, and MET165
Stigmasta7,22-dien-3β,4β-diol	-8.61	THR26	2.61 and 3.40	HIS41 (Pi- Sigma)	LEU27, HIS41, MET49, CYS145, and MET165
α-hederine	-8.14	THR24 THR26 ASN142 HIS164 GLU166	2.99 3.06 4.35 2.72 2.56 and 3.46	HIS41 (Pi- Sigma	MET49
Inermidioic acid	-8.05	ASN142 CYS145	2.87 2.74	HIS41 (Pi- Anion) and HIS163 (Pi-Anion)	Met49 and CYS145

continued

Table 1 Continued

Compounds	Free binding energy (kcal/mol)	Molecular interactions analysis within the 3CLpro active binding site			
		H-bond	Distance (Å)	Pi-Sigma / Pi-Anion	Hydrophobic interaction
Michael acceptor inhibitor (N3)	-5.49	ASN142 GLY143, GLN189	2.89 2.62 3.04		LEU27, HIS41, CYS145, HIS163, AND met165

Note: Table 1 Molecular docking scores (free binding energy in kcal/mol) for the phytochemical compounds lensoside Aβ, persicoside D, 2",2"'-di-O-α-rhamnopyranosyl-vicenin II, quercetin-7-O- rutinoside, officinoterpenoside E, basilmoside 24-ethyl-25-methylcholesta-5,22-dien-3–β-O-D- glucoside, apigenin 7-O-β-D-apiofuranosyl(1→2)–β–D-glucopyranoside, racemosol, stigmasta-7,22- dien-3β,4β-diol, α-hederine, inermidioic acid, and the co-crystallized ligand Michael acceptor inhibitor (N3) against the SARS-CoV-2 main protease ($3CL^{pro}$) (PDB ID: 6LU7). The compounds are listed from the lowest (more negative) to the highest (less negative) free binding energy values. The table also includes an analysis of the 2D molecular interactions between these compounds and the residues within the $3CL^{pro}$ active site

Table S1 Overview of the 42 medicinal plants and their bioactive compounds screened for inhibition of SARS-CoV-2 $3CL^{pro}$. The table presents molecular docking scores (free binding energy in kcal/mol) for each compound, including those with stronger binding affinities than the reference inhibitor N3

No	Medicinal plants	Constituent	Free binding energy (kcal/mol)	References
1	*Euphorbia neriifolia*	β–friedelanol	-4.28	(Chang et al. 2012)
		β–acetoxy friedelane	-4.30	
		Friedelin	-3.89	
		Epitaraxerol	-4.13	
2	*Euphorbia hirta*	Afzelin	-5.04	(Gyuris et al. 2009)
		Quercitin	-3.13	
		Myricitrin	-5.47	
		α–amyrin	-5.17	
		β–amyrin	-5.26	
		Friedelin	-3.89	
		Taraxerol	-4.32	
3	*Andrographis paniculata*	Andrographolide	-4.90	(Wiart et al. 2005, Tang et al. 2012)
		Neoandrographolide	-5.67	
		14-deoxy-11,12-didehydroandrographolide	-4.70	
4	*Momordica charanthia*	Kuguacin C	-4.92	(Bourinbaiar and Lee-Huang 1996, Tang et al. 2012),
		Kuguacin E	-4.85	
		Momordicine I	-3.87	
5	*Leucaena*	Galactomanan	-3.62	(Ono et al. 2003

continued

Table S1 Continued

No	Medicinal plants	Constituent	Free binding energy (kcal/mol)	References
6	*Psidium guajava*	Gallic acid	-0.99	(Sriwilaijaroen et al. 2012)
		Catechin	-3.09	
		Quercetin	-3.15	
		Guajaverin	-5.22	
		Avicularin	-5.27	
7	*Morinda elliptica*	Nordamnacanthal	-3.38	(Hamidi et al. 1996)
		Damnacanthal	-3.73	
		Morindone	-2.87	
8	*Piper sarmentosum*	Pellitorine	-4.42	(Hussain et al. 2012)
		Guineensine	-4.84	
		Brachystamide B	-5.49	
		Sarmentine	-3.71	
		Brachyamide B	-5.49	
		1-piperettyl pyrrolidine	-4.61	
		3',4',5'-Trimethoxycinnamoyl pyrrolidine	-3.02	
		Sarmentosine	-3.30	
9	*Trichosnathes kirilowii*	Trichosanthin	-2.79	(Chen et al. 2006)
10	*Morinda citrifolia*	Americanin A	-4.91	(Hayashi et al. 1995, Choi et al. 2009, Chiow et al. 2016)
		Narcissoside	-4.84	
		Asperuloside	-4.49	
		Asperulosidic Acid	-4.73	
		Borreriagenin	-2.64	
		Citrifolinin B epimer a	-4.57	
		Citrifolinin B epimer	-4.94	
		Nicotifloroside	-3.39	
		Scopoletin	-1.66	
		Ursolic acid	-4.49	
11	*Houttuynia cordata*	Quercetin	-3.15	(Hayashi et al. 1995, Choi et al. 2009, Chiow et al. 2016)
		Quercetrin	-3.89	
		Cinanserin	-1.36	
		Quercetin 3-rhamnoside	-4.52	
		Methyl n-nonyl ketone	-1.36	
		Lauryl aldehyde	-2.43	
		Capryl aldehyde	-1.36	

continued

Table S1 Continued

No	Medicinal plants	Constituent	Free binding energy (kcal/mol)	References
12	*Lobelia chinensis*	Lobechine	-3.45	(Kuo et al. 2011)
		Scoparone	-2.19	
13	*Elephantopus scabe*	1α,2β–O– dicaffeoylcyclo-pentan-3β–ol	-4.62	(Geng et al. 2011)
		Dicaffeoylquinic acids	-4.81	
14	*Calotropis gigantean*	Lignan glycoside	-4.12	(Parhira et al. 2014)
		(+)-pinoresinol 4-O-[6″-O-vanilloyl]-β-D-glu-copyranoside	-3.62	
15	*Melastoma malabathricum*	Quercetin	-3.15	(Joffry et al. 2012
		Quercetrin	-3.89	
		Rutin	-5.12	
16	*Asplenium nidus*	Gliricidin-7-O-hexoside	-4.86	(Tahir et al. 2014)
		Quercetin-7-O-rutinoside	-8.97	
17	*Eleusine indica*	3-O-β-d-glucopyranosyl stig-masterol	-4.71	(Tahir et al. 2014, Iberahim et al. 2015
18	*Phaleria macrocarpa*	Kaempferol-3-o–β-D-glucoside	-5.79	(Tahir et al. 2014)
		Dodecanoic acid	-3.64	
		Palmitic acid	-4.92	
		Icariside II	-3.54	
		Mangiferin	-4.61	
		Gallic acid	-0.99	
19	*Nigella sativa L.*	Dithymoquinone	-5.02	(Ulasli et al. 2014)
		Thymol	-1.13	
		Thymohydroquinone	-3.11	
		β-pinene	-2.89	
		d-Limonene	-3.20	
		d-Citronellol	-3.26	
		p-Cymene	-4.19	
		Carvacrol	-4.61	
		t-Anethole	-1.64	
		4-Terpineol	-4.01	
		nigellicine	-3.46	
		Nigellidine	-3.41	
		α-Hederine	-8.14	

continued

Table S1 Continued

No	Medicinal plants	Constituent	Free binding energy (kcal/mol)	References
20	*Camellia sinensis*	Caffeine	-3.07	(Mahmood et al. 2016)
		Gallic acid	-0.99	
		Catechin	-3.09	
		Ampelopsin	-3.24	
		Epicatechin	-3.07	
		(-)-epiafzelechin	-3.05	
		Theflavin	-4.88	
		Isotheflavin	-2.54	
		Theflavic acid	-3.26	
		Theobromine	-2.86	
		Theophylline	-0.35	
		xanthine	-0.33	
21	*Durio zibenthinus*	p-Coumaric acid	-0.94	(Nikomtat et al. 2017)
		Ferulic acid	-2.24	
		p-Anisic acid	-1.15	
		Gallic acid	-0.99	
		Vanillic acid	-0.93	
		Rutin	-5.12	
		Quercetin	-3.15	
		Morin	-3.25	
		Myrectin	-3.46	
		Kaempferol	-3.14	
		Fraxidin	-2.86	
		Eucryphin	-4.04	
		Boehmenan	-4.21	
22	*Cinnamomum zeylanicum Blume*	Cinnamaldehyde	-1.01	(Fabros Jr et al. 2018)
		trans-Caryophyllene	-1.71	
		Eugenol	-2.30	
		Hydrocinnamic acid	-1.65	
		trans-Cinnamyl acetate	-2.33	
		Coumaric acid	-1.79	
		Propenoic acid	-0.94	
		δ-Cadinene	-2.29	
		Caryophyllene oxide	-1.80	
		Naphthalenol	-0.79	
		n-Hexadecanoic Acid	-4.81	
		9-Octadecenoic acid	-4.64	
		Phthalic acid	-1.69	
		1,4-Benzenedicarboxylic acid	-3.81	

continued

Table S1 Countinued

No	Medicinal plants	Constituent	Free binding energy (kcal/mol)	References
23	*Cocos nucifera*	Catechin	-3.09	(Esquenazi et al. 2002)
		Epicatechin	-3.07	
		Lupeol	-4.31	
		Skimmiwallin	-4.88	
		Isoskimmiwallin	-3.67	
24	*Cymbopogon schoenanthus*	Cassiaoccidentalin B	-4.65	(Khalil et al. 2017)
		Luteolin	-3.08	
		d-Limonene	-1.00	
		Geraniol	-2.14	
		Isoorientin	-5.14	
		Isoscoparin	-5.29	
		Swertiajaponin	-4.81	
		Chlorogenic acid	-4.32	
		Caffeic acid	-1.69	
		Orientin	-4.93	
		Geranic acid	-2.08	
25	*Citrullus lanatus*	lanatusosides C	-4.93	(Omigie and Agoreyo 2014)
		Lanatusosides D	-4.91	
		Cucurbitacin B	-4.60	
		Cucurbitacin E	-4.77	
26	*Phoenix dactylifera*	β-sitosterol	-1.70	(Jassim and Naji 2010)
		Protocatechuic acid	-1.77	
		p-hydroxybenzoic acid	-0.78	
		Luteolin	-0.80	
		Diosmetin 7-ObL-arabinofuranosyl (1→2) bD-apiofuranoside	-3.21	
		Clionasterol acetate	-5.32	
		Cholesterol	-5.79	
		Estrone	-5.22	
		Estradiol	-3.99	
		Apigenin	-3.78	
		Naringin	-3.41	
27	*Allium cepa*	Kaempferol	-3.14	(Romeilah et al. 2010, Harazem et al. 2019)
		Quercetin	-3.15	
		Isorhamnetin	-3.23	
		Cyanidine	-4.11	
		Peonidin	-4.24	
		(+)-S-Methyl-L-cysteine sulphoxide	-2.17	
		(+)-S-propyl-L-cysteine sulphoxide	-1.10	

continued

Table S1 Continued

No	Medicinal plants	Constituent	Free binding energy (kcal/mol)	References
28	*Solanum melongena*	Officinoterpenoside E	-8.91	(Di Sotto et al. 2018)
		Arjunolic acid	-5.92	
		Corchoionol C	-3.42	
		Syringaresinol	-4.17	
		Buddlenol A	-5.98	
		N-trans-p-coumaroyloctopamine	-4.82	
		Solasodine	-4.84	
29	*Allium sativum*	Alliin	-2.30	(Romeilah et al. 2010)
		Allicin	-1.10	
		Trigonelline	-0.94	
		Proto-iso-eruboside B	-3.57	
		Eruboside-B	-4.16	
		Isoeruboside B	-4.67	
30	*Lawsonia inermis*	Lawsoinermone	-2.26	(Mouhajir et al. 2001)
		Inermidioic acid	-8.05	
		Inermic acid	-3.93	
		7-hydroxy-3,5-dimethoxy-6,8-dimethylflavone	-3.69	
		Eudesmane-4β,7α-diol	-2.74	
31	*Trigonella foenumgraecum*	4-Hydroxyisoleucine	-1.37	(Hussein et al. 2000)
		Diosgenin	-4.05	
		Yamogenin	-4.60	
		Fenugreekine	-4.57	
		Vicenin-1	-5.60	
		Isoschaftoside	-5.29	
		Schaftoside	-4.94	
		Trigonelline	-0.94	
		Carpaine	-4.92	
		Naringenin	-2.85	
		Kaempferol-3-o-β-D-glucoside	-5.79	
		Apigenin-6-C-glucoside	-3.60	
32	*Ocimum basilicum*	2-phenyl-2,3-dihydrochromen-4-one	-2.11	(Chiang et al. 2005)
		2-4-(benzyloxy-3-methoxyphenyl)-2-3-dihydrochromen-4-one	-4.67	
		Basilmoside 24-ethyl-25-methylcholesta-5,22- dien-3-β-O-D-Glucoside	-8.87	
		Betulinic acid	-4.63	
		Oleanolic acid	-4.01	

continued

Table S1 Continued

No	Medicinal plants	Constituent	Free binding energy (kcal/mol)	References
		Ursolic acid	-4.49	
		3-epimaslinic acid	-4.7	
		Alphitolic acid	-4.48	
		Euscaphic acid	-4.16	
		Ferulic acid	-2.24	
		P-coumaric acid	-0.94	
		Caffeic acid	-1.69	
		Cinnamic acid	-1.80	
		Kaempferol	-3.14	
		Quercetin	-3.15	
		Ellagic acid	-1.61	
		Chlorogenic acid	-4.32	
		Catechin	-3.09	
33	*Zingiber officinalle*	5-hydroxy-1-(4-hydroxy-3-methoxyphenyl)tetradecan-4,8-dien-3-One	-4.95	(San Chang et al. 2013)
		5-hydroxy-1-(4-hydroxy-3-methoxyphenyl)hexadecan-4,10-dien-3-one	-3.73	
		5-hydroxy-1-(4-hydroxy-3-methoxyphenyl)hexadec-4-en-3-one	-4.25	
		5-hydroxy-1-(4-hydroxy-3-methoxyphenyl)eicos-4,11,14-trien-3-one	-3.75	
		1-(4-hydroxy-3-methoxyphenyl)eicos-4,11,14-trien-3-one	-4.40	
		1-(4-methoxy-3-hydroxyphenyl)-3-(4-nonanyl furan-1-yl) propan-3-one	-4.93	
		4-shogaol	-4.57	
		6-shogaol	-4.94	
		8-shogaol	-4.55	
		10-shogaol	-4.28	
		12-shogaol	-4.78	
34	Senna alexandrina	2,5-dimethyl-4-hydroxy-3(2H)-furanone	-0.88	(Ikram et al. 2023)
		2-propyl-tetrahydropyran-3-ol	-0.90	
		Estragole	-0.07	
		1-ethynyl-4-fluoro Benzene	-0.03	

continued

Table S1 Continued

No	Medicinal plants	Constituent	Free binding energy (kcal/mol)	References
		5-Hydroxymethylfurfural	-0.99	
		Anethole	-1.07	
		2-Methoxy-4-vinylphenol	-2.26	
		1,2,2-trimethylcyclopentane1,3-dicarboxylic acid	-4.02	
		Tetradecenoic acid	-2.18	
		Caryophyllene	-5.39	
		2-Methylenecholestan-3-ol	-3.40	
		1-(1,5-dimethyl-4- hexen-yl)-4-methyl benzene	-3.31	
		Alpha-Curcumene	-3.86	
		Beta-Curcumene	-3.51	
		7-epi-cis-sesquisabinene hydrate	-2.09	
		Beta-Sesquiphellandrene	-3.90	
		Desulphosiniqrin	-3.15	
35	*Beta vulgaris*	2”,2”’-di-O-α- rhamnopyranosyl-vicenin II	-9.22	(Betancur-Galvis et al. 1999)
		Herbacetin 3-O-β- xylopyranosyl-(1”’→2”)- O-β-glucopyranoside	-4.03	
36	*Hordeum vulgare*	Tricin	-3.89	(Sinha et al. 2012
		Gallocatechin	-3.64	
		Catechin	-3.09	
		Epicatechin	-3.07	
		Procyanidin B3	-4.62	
		Prodelphinidin B3	-4.44	
37	*Musa acuminata*	Umbelliferone	-1.08	(de Camargo et al. 2020)
		31-norcyclolaudenone	-5.76	
		Cycloartenol	-4.16	
		24-trimethyl-5a-cholesta-8,25(27)-dien-3b-ol	-5.13	
		4-Epicyclomusalenone	-5.51	
		Cycloeucalenol acetate	-5.24	
38	*Lens culinaris*	Lensoside Aβ	-9.88	(Chatzivassiliou et al. 2016, Wang et al. 2021)
		Keto-2-hydroxyglycitein	-3.10	
		Stachyose	-3.26	
		Arbutin	-3.17	
		Hypaphorine	-5.17	
		4-chloro-1H-indole-3-N-methylacetamide	-3.17	

continued

Table S1 Continued

No	Medicinal plants	Constituent	Free binding energy (kcal/mol)	References
39	*Apium graveolens*	Luteolin 7-O-[β-D- apiofuranosyl(1→2)-(6″- O-malonyl)]-β-D- glucopyranoside	-4.08	(Choochote et al. 2004)
		Apigenin 7-O-[β– Dapiofuranosyl(1→2)-(6″– O-malonyl)]–β-D- glucopyranoside	-4.81	
		Chrysoeriol 7-O-β– Dapiofuranosyl(1→2)-β- D-glucopyranoside	-5.84	
		Apigenin 7-O-β-D-apiofuranosyl(1→2)-β-D- glucopyranoside	-8.76	
		Luteolin 7-O–β-D- apiofuranosyl(1→2)-β–D- glucopyranoside	-4.60	
		Luteolin 7-O-β-D- glucopyranoside	-4.51	
		Butylphthalide	-2.14	
		Senkyunolide A	-4.81	
		Sedanolide	-4.81	
		p-hydroxyphenethyltrans-ferulate	-4.71	
		Bergapten	-1.73	
		Scopoletin	-4.81	
40	*Allium porrum*	Persicoside A	-4.97	(Keyaerts et al. 2007, Chen et al. 2011)
		Persicoside B	-4.97	
		Persicoside C	-5.22	
		Persicoside D	-9.27	
		Persicoside E	-4.05	
		Persicoimidate	-5.97	
		N-feruloyl tyramine	-4.49	
41	*Curcuma longa*	o-Cymene	-0.86	(Ichsyani et al. 2017)
		4-isopropenyl-1,2- dimethyl-cyclohexan2-enol	-1.97	
		2-ethenyl-1,1- dimenthyl-3-methylene-cyclohexane	-1.26	
		α–Thujone	-1.40	
		cis-Sabinol	-1.85	
		2-isopropylidene3-methylhexa-3,5- dienal	-1.76	
		2-methoxy-4-vinylphenol	-1.53	
		m-Eugenol	-2.02	
		Hemellitol	-0.99	
		α-Cedrene	-1.22	

continued

Table S1 Continued

No	Medicinal plants	Constituent	Free binding energy (kcal/mol)	References
		β-caryophyllene	-0.98	
		β-bisabolene	-1.59	
		β-vatirenene	-1.90	
		β-tumerone	-1.74	
		Curcumin	-5.03	
42	*Lagenaria siceraria*	4-hydroxymethyl-phenyl-6-O-caffeoyl-b-D- glucopyranoside	-4.14	(Kumar et al. 2015)
		3,4-dimethoxy cinnamic acid	-4.18	
		Campesterol	-5.21	
		Racemosol	-8.66	
		Stigmasterol	-4.56	
		Stigmasta7,22-dien-3β,4β-diol	-8.61	

Following the validation, the docking of the selected phytochemical compounds revealed several candidates with binding energies lower than -2 kcal/mol compared to N3, indicating stronger interactions with $3CL^{pro}$ (Al-Thiabat et al. 2021b, Amir Rawa et al. 2022, Shalayel et al. 2020). Compounds with more negative binding energies were considered for further analysis. Among these, the top 11 compounds included lensoside Aβ (-9.88 kcal/mol), persicoside D (-9.27 kcal/mol), 2",2"'-di-O-α–rhamnopyranosyl-vicenin II (-9.22 kcal/mol), quercetin-7-O-rutinoside (-8.97 kcal/mol), officinoterpenoside E (-8.91 kcal/mol), basilmoside 24-ethyl-25-methylcholesta-5,22-dien-3-β-O-D-glucoside (-8.87 kcal/mol), apigenin 7-O-β-D-apiofuranosyl (1→2)-β-D-glucopyranoside (-8.76 kcal/mol), racemosol (-8.66 kcal/mol), stigmasta-7,22-dien-3β,4β-diol (-8.61 kcal/mol), α-hederine (-8.14 kcal/mol), and inermidioic acid (-8.05 kcal/mol). The molecular interactions and binding energies of these compounds are detailed in Table 1 and Figure 2.

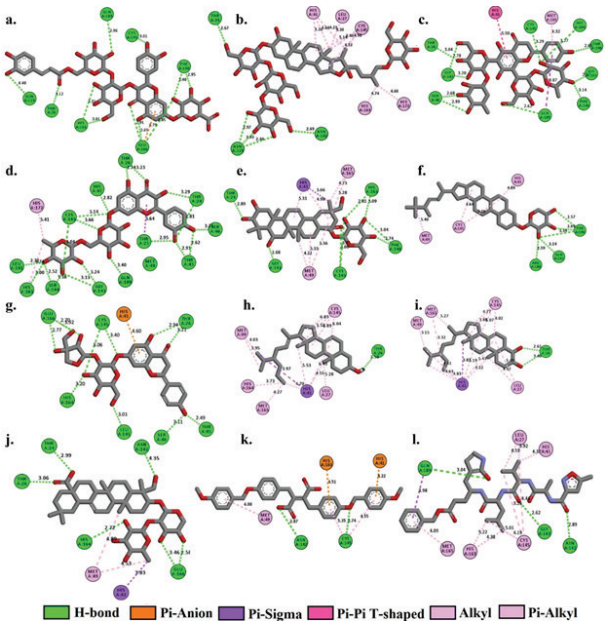

Figure 2 2D binding interactions between the SARS-CoV-2 main protease (3CLpro) (PDB ID: 6LU7) and various phytochemicals, including lensoside Aβ (a), persicoside D (b), 2",2"'-di-O-α-rhamnopyranosyl vicenin II (c), quercetin-7-O-rutinoside (d), officinoterpenoside E (e), basilmoside 24-ethyl-25-methylcholesta-5,22-dien-3–β-O-D-glucoside (f), apigenin 7-O-β-D-apiofuranosyl(1→2)-β-D-glucopyranoside (g), racemosol (h), stigmasta-7,22-dien-3β,4β-diol (i), α–hederine (j), inermidioic acid (k), and the co-crystallized ligand, Michael acceptor inhibitor (N3) (l)

Lensoside Aβ demonstrated several key interactions within the 3CL^{pro} active site. Hydrogen bonds were formed with residues THR26 (3.12 Å), ASN119 (4.40 Å), PHE140 (2.95 and 3.40 Å), CYS145 (3.01 Å), HIS164 (3.01 and 3.31 Å), GLU166 (2.65, 2.85, and 2.91 Å), and GLN189 (2.96 Å). Additionally, a Pi-anion interaction was observed with GLU166. The significant interaction with HIS41 and CYS145, part of the catalytic dyad of 3CL^{pro}, indicates a strong potential for inhibiting the protease, much like N3, which also interacts with CYS145 (Ferreira et al. 2021, Shalayel et al. 2020, Zanetti-Polzi et al. 2021). The multiple hydrogen bonds and Pi-anion interaction suggest that lensoside Aβ may be a potent inhibitor, with interactions closely resembling the nature of the active site residues. Similarly, persicoside D formed hydrogen bonds with THR24 (2.67 Å), ASN119 (2.44, 2.97, and 3.03 Å), and ASN142 (2.69 Å). It also exhibited hydrophobic interactions with residues LEU27, HIS41, CYS145, HIS163, and HIS172. The interaction with HIS41 and CYS145 are particularly noteworthy, as it is crucial for the enzyme's catalytic function (Ferreira et al. 2021, Shalayel et al. 2020, Zanetti-Polzi et al. 2021). The combination of hydrogen bonding and hydrophobic interactions, especially with catalytic residues, makes persicoside D a promising candidate for further investigation.

2",2"'-di-O-α-rhamnopyranosyl-vicenin II formed hydrogen bonds with THR26 (3.04 Å), SER46 (2.68 and 2.99 Å), PHE140 (3.14 Å), GLY143 (2.78 and 3.2 Å), CYS145 (3.29 Å), HIS163 (2.97 Å), HIS164 (3.27 Å), GLN189 (2.62 Å), and THR190 (2.69 Å). A Pi-sigma interaction was observed with GLN189, while hydrophobic interactions occurred with HIS41 and MET165. The involvement of key residues such as CYS145 and HIS41 in both hydrogen bonding and hydrophobic interactions suggests that 2",2"'–di–O–α–rhamnopyranosyl-vicenin II could effectively inhibit 3CL^{pro} by stabilising the enzyme-inhibitor complex, similar to the mechanism observed with N3. Quercetin-7-O-rutinoside formed multiple hydrogen bonds with THR24 (2.81 and 3.29 Å), THR25 (2.95 Å), THR26 (2.74 and 3.23 Å), HIS41 (2.82 Å), THR45 (2.62 and 2.91 Å), SER46 (3.15 Å), LEU141 (2.71 Å), GLY143 (3.13 and 3.24 Å), SER144 (2.52 and 3.38 Å), CYS145 (3.14, 3.04, and 3.66 Å), HIS163 (3.00 Å), and GLN189 (3.40 Å). It also exhibited Pi-sigma interactions with THR25 and hydrophobic interactions with HIS163 and HIS172. The involvement of multiple hydrogen bonds with CYS145 and HIS41, alongside its favourable Pi interactions, suggests that quercetin–7–O–rutinoside may have potential as a 3CL^{pro} inhibitor.

Officinoterpenoside E formed hydrogen bonds with THR24 (2.89 Å), PHE140 (2.74 and 3.04 Å), GLY143 (2.68 Å), CYS145 (3.06 and 3.75 Å), and HIS163 (2.81 and 3.09 Å). A Pi-sigma interaction was observed with HIS41, and hydrophobic interactions occurred with HIS41, MET49, and MET165. The presence of multiple interactions with key residues such as CYS145 and HIS41, as well a map of hydrophobic interactions, indicates that officinoterpenoside E has a binding pattern similar to N3 and could potentially act as a potent inhibitor. Basilmoside 24-ethyl-25-methylcholesta-5,22-dien-3-β-O-D-glucoside created hydrogen bonds with ARG188 (2.59 Å), THR190 (2.57, 2.69, and 3.39 Å), and GLN192 (3.14 Å). Hydrophobic interactions were observed with HIS41, MET49, and CYS145. Despite fewer hydrogen bonds, the involvement of CYS145 and HIS41 in hydrophobic interactions suggests that basilmoside 24-ethyl-25-methylcholesta-5,22-dien-3–β–O–D-glucoside may still effectively bind to the 3CL^{pro} active site and inhibit its activity.

Apigenin 7–O–β–D–apiofuranosyl (1→2)-β–D–glucopyranoside formed hydrogen bonds with THR26 (2.94 and 3.21 Å), THR45 (2.49 Å), SER46 (3.11 Å), LEU141 (3.01 Å), CYS145 (3.06 and 3.40 Å), HIS164 (3.20 Å), and GLU166 (2.70, 2.77, and 3.92 Å). A Pi-anion interaction was observed with HIS41, suggesting strong binding stability, especially through its interaction with the key residue CYS145, which parallels the inhibitory mechanism of N3. Racemosol formed hydrogen bonds with THR26 (2.59 Å) and displayed Pi-sigma interactions with HIS41. Hydrophobic interactions were observed with LEU27, HIS41, MET49, CYS145, HIS164, and MET165. These interactions suggest strong binding affinity, particularly through its hydrophobic interactions with the catalytic dyad (HIS41 and CYS145), making racemosol a strong candidate for further study. Stigmasta-7,22-dien-3β,4β-diol formed hydrogen bonds with THR26 (2.61 and 3.40 Å)

and exhibited Pi-sigma interactions with HIS41. Hydrophobic interactions were observed with LEU27, HIS41, MET49, CYS145, and MET165, indicating a stable binding conformation similar to N3 and further supporting its potential as a $3CL^{pro}$ inhibitor.

α–Hederine formed hydrogen bonds with THR24 (2.99 Å), THR26 (3.06 Å), ASN142 (4.35 Å), and HIS164 (2.72 Å). Pi-sigma interactions were observed with HIS41, and hydrophobic interactions with MET49. The involvement of key residues such as HIS41 and CYS145 suggests that α–hederine may have a similar inhibitory mechanism to N3, but further validation is necessary to confirm its potential. Finally, inermidioic acid created hydrogen bonds with ASN142 (2.87 Å) and CYS145 (2.74 Å). Pi-anion interactions were observed with HIS41 and HIS163, while hydrophobic interactions occurred with MET49 and CYS145. The strong interaction with CYS145 and Pi-anion interactions with HIS41 suggest that inermidioic acid could serve as an effective $3CL^{pro}$ inhibitor, similar to N3.

DISCUSSION

Lensoside Aβ, derived from Lens culinaris (lentils), exhibited the strongest binding energy of -9.88 kcal/mol and demonstrated significant interactions with key residues in the 3CLpro active site, including CYS145, HIS164, and GLN189. Lentils are well-known for their rich nutritional profile and antioxidant properties, contributing to overall health and immune support (Riaz et al. 2024). A study by Prashanth et al. (2024) highlighted the anti-inflammatory and antioxidant properties of Lens culinaris, which could complement the antiviral potential of lensoside Aβ. The strong hydrogen bonding and Pi-anion interactions with GLU166 suggest that this compound could effectively inhibit the enzymatic activity of $3CL^{pro}$. Therefore, Lens culinaris, with its nutritional and bioactive properties, can be explored as part of a natural therapeutic strategy during COVID-19 treatment, particularly due to lensoside Aβ's strong inhibitory interactions with the $3CL^{pro}$ active site.

Similarly, persicoside D, isolated from Allium ampeloprasum (leek), displayed a binding energy of -9.27 kcal/mol and formed critical hydrogen bonds with THR24, ASN119, and ASN142. Allium ampeloprasum has been studied for its antioxidant and immune-boosting effects, with previous research indicating its use in traditional remedies for respiratory and viral infections (Yan et al. 2023). Additionally, it engaged in hydrophobic interactions with LEU27, HIS41, and CYS145, key residues involved in the catalytic function of $3CL^{pro}$. Given the immune-boosting and antimicrobial properties of Allium ampeloprasum, persicoside D could serve as a complementary treatment in managing viral replication during COVID-19, especially in strengthening the body's natural defenses against viral infections.

2",2"'-Di-O–α–rhamnopyranosyl vicenin II, found in Beta vulgaris (beetroot), also exhibited strong binding with $3CL^{pro}$, with a binding energy of -9.22 kcal/mol. This compound formed multiple hydrogen bonds with crucial residues such as CYS145, HIS163, and GLY143, alongside Pi-sigma interactions with GLN189. Beta vulgaris is rich in bioactive compounds, known for their antioxidant, anti-inflammatory, and immune-modulating properties (Varshney & Mishra 2022). Recent research by Ritz et al. (2021) suggested that beetroot extracts could enhance immune function and protect against oxidative stress, which is crucial in combating viral infections. The potential of 2",2"'-di-O-α–rhamnopyranosyl vicenin II as a 3CLpro inhibitor suggests that consuming Beta vulgaris or using its extracts could offer a natural therapeutic advantage in fighting COVID-19 by directly inhibiting the viral protease and supporting the immune system.

Quercetin-7-O-rutinoside, isolated from Asplenium nidus, had a binding energy of -8.97 kcal/mol and demonstrated interactions with several important residues, including CYS145, HIS163, and GLN189. Studies have long established quercetin as a potent antiviral agent, capable of inhibiting the replication of various viruses, including influenza and herpes simplex virus (Agrawal et al. 2020, Behl et al. 2021, Carrillo-Martinez et al. 2024). It also formed Pi-sigma interactions with THR25 and hydrophobic contacts with HIS172, further stabilizing its binding. Asplenium nidus has traditionally been used for its anti-inflammatory properties, and the presence of quercetin-

7-O-rutinoside in this plant strengthens its potential as a therapeutic agent in COVID-19 management (Ali & Abdulwahab 2024). The ability of quercetin derivatives to inhibit viral enzymes and modulate immune responses makes Asplenium nidus a promising candidate for further exploration in combating SARS-CoV-2.

Officinoterpenoside E, sourced from Solanum melongena (eggplant), showed strong binding energy at -8.91 kcal/mol, interacting with key $3CL^{pro}$ residues such as CYS145 and HIS163. Eggplant extracts have been studied for their anti-inflammatory, antioxidant, and antimicrobial properties (Bouhajeb et al. 2020, Zearah 2024), and research has pointed to its bioactive compounds having protective effects against respiratory infections (Govender et al. 2022). Officinoterpenoside E also formed Pi-sigma interactions with HIS41 and hydrophobic interactions with MET49 and MET165, indicating its potential to disrupt the viral protease's function. Given the health-promoting properties of Solanum melongena and the significant molecular interactions of officinoterpenoside E, this compound could be explored further as an effective natural inhibitor of SARS-CoV-2 replication.

Basilmoside 24-ethyl-25-methylcholesta-5,22-dien-3-β-O-D-glucoside, from Ocimum basilicum (basil), exhibited a binding energy of -8.87 kcal/mol and formed key hydrogen bonds with ARG188 and THR190. Ocimum basilicum has been traditionally used for its antiviral, anti-inflammatory, and antioxidant properties, with studies demonstrating its efficacy against respiratory viruses like influenza and RSV (Bhattacharya et al. 2024, Venu & Austin 2020). The compound also engaged in hydrophobic interactions with HIS41 and CYS145, critical for inhibiting $3CL^{pro}$. The antiviral and anti-inflammatory properties of Ocimum basilicum make it an attractive candidate for further investigation in COVID-19 treatment, particularly for its potential role in inhibiting viral replication and alleviating respiratory symptoms.

Apigenin 7-O-β-D-apiofuranosyl(1→2)-β-D-glucopyranoside, from Apium graveolens (celery), displayed a binding energy of -8.76 kcal/mol and interacted with key residues such as CYS145, HIS164, and GLU166. Apigenin, a well-known flavonoid, has been documented for its anti-inflammatory and antiviral properties, with studies highlighting its ability to inhibit viral replication in dengue, influenza, and other viruses (Zakaryan et al. 2017). Pi-anion interactions were also observed with HIS41, indicating strong binding stability. Apium graveolens has been used in traditional medicine for its immune-boosting and anti-inflammatory effects (Dogara et al. 2023), making it a valuable plant to explore in therapeutic strategies for managing COVID-19.

Interestingly, the results showed that both racemosol and stigmasta-7,22-dien-3β,4β-diol, derived from the same plant, Lagenaria siceraria (bottle gourd), exhibited strong binding affinities with $3CL^{pro}$, with binding energies of -8.66 kcal/mol and -8.61 kcal/mol, respectively. Racemosol interacted with key $3CL^{pro}$ residues, including CYS145, HIS41, and MET49, and demonstrated a strong Pi-sigma interaction with HIS41, suggesting its potential as a stable inhibitor of the protease. Similarly, stigmasta-7,22-dien-3β,4β-diol engaged in both Pi-sigma and hydrophobic interactions with the same critical residues, indicating its inhibitory potential. Lagenaria siceraria has been traditionally used to treat respiratory illnesses, and recent studies have highlighted its anti-inflammatory, hepatoprotective, and antiviral properties (Roy et al. 2022, Saeed et al. 2022), making it a promising candidate for further research in the context of COVID-19 therapy.

α-Hederine, sourced from Nigella sativa (black cumin), exhibited a binding energy of -8.14 kcal/mol and formed hydrogen bonds with THR24, THR26, and HIS164, along with Pi-sigma interactions with HIS41. Nigella sativa has been widely recognised for its immune-boosting and antiviral properties, with numerous studies documenting its use in respiratory infections, including asthma and bronchitis (Hussain et al. 2024, Ojueromi et al. 2022). The molecular interactions of α-Hederine with $3CL^{pro}$ reinforce its potential as a natural antiviral agent for COVID-19 treatment, particularly for its ability to modulate immune responses and directly inhibit viral replication.

Lastly, inermidioic acid, isolated from Lawsonia inermis (henna), displayed a binding energy of -8.05 kcal/mol, forming hydrogen bonds with ASN142 and CYS145, and Pi-anion

interactions with HIS41 and HIS163. Lawsonia inermis has been traditionally used for its antimicrobial, antiviral, and anti-inflammatory effects, with studies showing its efficacy against various viral pathogens (Singam et al. 2020). The strong binding of inermidioic acid with critical $3CL^{pro}$ residues suggests that it could be explored as a natural inhibitor of SARS-CoV-2, supporting the use of Lawsonia inermis in complementary COVID-19 therapies aimed at reducing viral load and alleviating symptoms.

This study provides preliminary insights into the potential use of phytochemical compounds and medicinal plants for the inhibition of SARS-CoV-2 main protease ($3CL^{pro}$). While the results from the in silico analysis are promising, it is important to acknowledge that they are theoretical and require further validation. Future studies should incorporate advanced computational methods, such as molecular dynamics simulations, to assess the stability and dynamics of the identified compounds within the binding site. Additionally, in vitro and in vivo experiments are necessary to validate the efficacy of these compounds and their potential as therapeutic agents. This would provide a more comprehensive understanding of their antiviral activity and pave the way for their development into clinical treatments.

CONCLUSION

In this study, eleven medicinal plants known for their bioactive compounds demonstrated strong inhibition of SARS-CoV-2 $3CL^{pro}$ compared to the reference inhibitor N3. The top compounds, including lensoside Aβ from Lens culinaris, persicoside D from Allium ampeloprasum, 2",2'''-di-O-α-rhamnopyranosyl vicenin II from Beta vulgaris, quercetin-7-O-rutinoside from Asplenium nidus, officinoterpenoside E from Solanum melongena, basilmoside from Ocimum basilicum, apigenin 7-O-β-D-apiofuranosyl glucopyranoside from Apium graveolens, racemosol and stigmasta-7,22-dien-3β,4β-diol from Lagenaria siceraria, α-hederine from Nigella sativa, and inermidioic acid from Lawsonia inermis, exhibited stronger binding affinities than N3. These findings suggest that these plants and their compounds could contribute to the prevention and management of COVID-19 as alternative therapies. However, our findings require further validation through in vitro assays, animal models, and ideally clinical trials to confirm their efficacy and safety in humans. The study underscores the potential of phytochemicals as alternative or complementary treatments for COVID-19 and other viral infections. Continued research in this area is essential to develop these promising compounds into effective natural antiviral agents, offering potential new therapeutic options in the ongoing fight against COVID-19 and emerging infectious diseases.

ACKNOWLEDGEMENT

The authors have no acknowledgements or funding to declare for this study.

REFERENCES

Afshar ZM, Ebrahimpour S, Javanian M et al. 2020. Coronavirus disease 2019 (COVID-19), MERS and SARS: Similarity and difference. *Journal of Acute Disease* 9: 194–199.

Agrawal PK, Agrawal C & Blunden G. 2020. Quercetin: antiviral significance and possible COVID-19 integrative considerations. *Natural Product Communications* 15: 1934578X20976293.

Akbulut E. 2022. Investigation of changes in protein stability and substrate affinity of 3CL-protease of SARS-CoV-2 caused by mutations. *Genetics and Molecular Biology* 45: e20210404.

Al-Thiabat, Gazzali A, Mohtar N et al. 2021a. Conjugated α-cyclodextrin enhances the affinity of folic acid towards FRα: molecular dynamics study. *Molecules* 26: 5304.

Al-Thiabat Mg, Saqallah FG, Gazzali AM et al. 2021b. Heterocyclic substitutions greatly improve affinity and stability of folic acid towards FRα. An in silico insight. *Molecules* 26: 1079.

Alhawarri M, Dianita R, Rawa M, Nogawa T & Wahab H. 2023a. Potential Anti-Cholinesterase Activity of Bioactive Compounds Extracted from Cassia grandis Lf and Cassia timoriensis DC. *Plants* 12: 344.

Alhawarri MB. 2024. Exploring the Anticancer Potential of Furanpydone A: A Computational Study on its Inhibition of MTHFD2 Across Diverse Cancer Cell Lines. *Cell Biochemistry and Biophysics* 1–18.

alhawarri MB, al-thiabat mg, dubey a et al. 2024a. ADME profiling, molecular docking, DFT, and MEP analysis reveal cissamaline, cissamanine, and cissamdine from Cissampelos capensis Lf as potential anti-Alzheimer's agents. *RSC Advances* 14: 9878–9891.

Alhawarri MB, Dianita R, Rawa Msa, Nogawa T & Wahab Ha. 2023b. Potential Anti-Cholinesterase Activity of Bioactive Compounds Extracted from *Cassia grandis* Lf and *Cassia timoriensis* DC. *Plants* 12:

344.

Alhawarri MB & Olimat S. 2024. Potential Serotonin 5-HT2A Receptor Agonist of Psychoactive Components of *Silene undulata* Aiton: LC-MS/MS, ADMET, and Molecular Docking Studies. *Curr. Pharm. Biotechnol.*

Ali H & Abdulwahab AQ. 2024. Potential of some therapeutic effect of Ruta *graveolenes* plant and their bioactivities: A review. *Medical Journal of Ahl al-Bayt University* 3: 174–189.

Alidmat MM, Alhawarri MB, Al-Refai M et al. 2024. Synthesis, Characterization and Glyoxalase inhibitory activity of 4, 6-Diheteroarylpyrimidine-2-amine derivatives: In vitro and in silico studies. *Egyptian Journal of Chemistry*

Alidmat MM, Khairuddean M, Kamal Nnsnm, Muhammad M, Wahab Ha, Althiabat Mg & Alhawarri Mb. 2022b. Synthesis, characterization, molecular docking and cytotoxicity evaluation of new thienyl chalcone derivatives against breast cancer cells. *Syst. Rev. Pharm* 13: 1.

Amir Rawa MS, Al-Thiabat MG, Nogawa T, Futamura Y, Okano A & Wahab H A. 2022. Naturally Occurring 8ß, 13ß-kaur-15-en-17-al and Anti-Malarial Activity from Podocarpus polystachyus Leaves. *Pharmaceutical* 15: 902.

Behl T, Rocchetti G, Chadha S Et Al. 2021. Phytochemicals from plant foods as potential source of antiviral agents: An overview. *Pharmaceuticals* 14: 381.

Betancur-Galvis L, Saez J, Granados H, Salazar A & Ossa J. 1999. Antitumor and antiviral activity of Colombian medicinal plant extracts. *Memórias do Instituto Oswaldo Cru*, 94: 531–535.

Bhattacharya R, Bose D, Maqsood Q, Gulia K & Khan A. 2024. Recent advances on the therapeutic potential with Ocimum species against COVID-19: A review. *South African Journal of Botany* 164: 188–199.

Biovia DS. 2017. *Discovery studio visualizer*. San Diego, CA, USA, 936.

Blankenship LR, Yang KS, Vulupala VR et al. 2024. SARS-CoV-2 Main Protease Inhibitors That Leverage Unique Interactions with the Solvent Exposed S3 Site of the Enzyme. A*CS Medicinal Chemistry Letters*

Boozari M & Hosseinzadeh H. 2021. Natural products for COVID–19 prevention and treatment regarding to previous coronavirus infections and novel studies. *Phytotherapy Research* 35: 864–876.

Bouhajeb R, Selmi S, Nakbi A et al. 2020. Chemical composition analysis, antioxidant, and antibacterial activities of eggplant leaves. *Chemistry & Biodiversity* 17; e2000405.

Bourinbaiar AS & Lee-Huang S. 1996. The Activity of Plant-Derived Antiretroviral Proteins MAP30 and GAP31 against Herpes Simplex Virus Infectionin Vitro. *Biochemical and Biophysical Research Communications* 219: 923–929.

Brodin P. 2021. Immune determinants of COVID-19 disease presentation and severity. *Nature Medicine* 27: 28–33.

Cannalire R, Cerchia C, Beccari AR, DI Leva FS & Summa V. 2020. Targeting SARS-CoV-2 proteases and polymerase for COVID-19 treatment: state of the art and future opportunities. *Journal of Medicinal Chemistry* 65: 2716–2746.

Carrillo-Martinez EJ, Flores-Hernández FY, Salazar-Montes AM, Nario-Chaidez Hf & Hernández-Ortega LD. 2024. Quercetin, a flavonoid with great pharmacological capacity. *Molecules* 29: 1000.

Chang FR, Yen Ct, Ei-Shazly M et al. 2012. Anti-human coronavirus (anti-HCoV) triterpenoids from the leaves of Euphorbia neriifolia. *Natural Product Communications* 7: 1934578X1200701103.

Chathappady House NN, Palissery S & Sebastian H. 2021. Corona viruses: a review on SARS, MERS and COVID-19. *Microbiology Insights* 14: 11786361211002481.

Chatzivassiliou EK, Giakountis A, Kumari SG & Makkouk KM. 2016. Viruses affecting lentil (*Lens culinaris* Medik.) in Greece; incidence and genetic variability of Bean leafroll virus and Pea enation mosaic virus. *Phytopathologia Mediterranea* 239–252.

Chaudhuri S, Symons JA & Deval J. 2018. Innovation and trends in the development and approval of antiviral medicines: 1987–2017 and beyond. *Antiviral Researc* 155: 76–88.

Chen Ch, Chou TW, Cheng LH & Ho CW. 2011. In vitro anti-adenoviral activity of five Allium plants. *Journal of the Taiwan Institute of Chemical Engineers* 42: 228–232.

Chen G, Huang W, Chen F & Shan J. 2006. Protective effects of trichosanthin in Herpes simplex virus-1 encephalitis in mice. *Zhongguo Dang dai er ke za zhi= Chinese Journal of Contemporary Pediatrics* 8: 239–241.

Chen X, Huang X, MA Q Et Al. 2024. Preclinical evaluation of the SARS-CoV-2 Mpro inhibitor RAY1216 shows improved pharmacokinetics compared with nirmatrelvir. *Nature Microbiology* 1–14.

Chiang LC, NG LT, Cheng Pw, Chiang W & Lin CC. 2005. Antiviral activities of extracts and selected pure constituents of Ocimum basilicum. *Clinical and Experimental Pharmacology and Physiology* 32: 811–816.

Chiow K, Phoon M, Putti T, Tan BK & Chow VT. 2016. Evaluation of antiviral activities of Houttuynia cordata Thunb. extract, quercetin, quercetrin and cinanserin on murine coronavirus and dengue virus infection. *Asian Pacific Journal of Tropical Medicine* 9: 1–7.

Choi HJ, Song JH, Park Ks & Kwon DH. 2009. Inhibitory effects of quercetin 3-rhamnoside on influenza A virus replication. *European Journal of Pharmaceutical Sciences* 37: 329–333.

Choochote W, Tuetun B, Kanjanapothi D et al. 2004. Potential of crude seed extract of celery, *Apium graveolens* L, against the mosquito *Aedes aegypti* (L.) (Diptera: Culicidae). *Journal of Vector Ecology* 29: 340–346.

Coerdt KM & Khachemoune A. 2021. Corona viruses: reaching far beyond the common cold. *African Health Sciences* 21: 207–13.

DE Camargo LJ, Picoli T, Fischer G et al. 2020. Antiviral activity of native banana lectin against bovine viral diarrhea virus and bovine alphaherpesvirus type 1. *International Journal of Biological Macromolecules*

DE Clercq E & LI G. 2016. Approved antiviral drugs over the past 50 years. *Clinical Microbiology Reviews* 29: 695–747.

DE Ruyck J, Brysbaert G, Blossey R & Lensink Mf. 2016. Molecular docking as a popular tool in drug design, an in silico travel. *Adv. Appl. Bioinform. Chem.* 1–11.

DE Vries M, Mohamed AS, Prescott RA et al. 2020. Comparative study of a 3CLpro inhibitor and remdesivir against both major SARS-CoV-2 clades in human airway models. *BioRxiv* 95: 1819–1820.

DE Vries M, Mohamed AS, Prescott RA Et Al. 2021. A comparative analysis of SARS-CoV-2 antivirals characterizes 3CLpro inhibitor PF-00835231 as a potential new treatment for COVID-19. *Journal of Virology* 95: 10.1128/jvi. 01819–20.

DI Sotto A, DI Giacomo S, Amatore D et al. 2018. A polyphenol rich extract from Solanum melongena L. DR2 peel exhibits antioxidant properties and anti-herpes simplex virus type 1 activity in vitro. *Molecules* 23: 2066.

Dogara A, Bello Ahmad N & Ishaq Jumare A. 2023. Medicinal Plants as A Natural Immune Booster. *Eurasian Journal of Science and Engineering* 9.

Dolinsky TJ, Czodrowski P, LI H Et Al. 2007. PDB2PQR: expanding and upgrading automated preparation of biomolecular structures for molecular simulations. *Nucleic Acids Research* 35: W522–W525.

Ebinger JE, Achamallah N, JI H et al. 2020. Pre-existing traits associated with Covid-19 illness severity. *PloS One* 15: e0236240.

EL Khoury M, Wanes D, Lynch-Miller M, Hoter A & Naim Hy. 2024. Glycosylation Modulation Dictates Trafficking and Interaction of SARS-CoV-2 S1 Subunit and ACE2 in Intestinal Epithelial Caco-2 Cells. *Biomolecules* 14: 537.

Esquenazi D, Wigg MD, Miranda MM Et Al. 2002. Antimicrobial and antiviral activities of polyphenolics from *Cocos nucifera* Linn.(Palmae) husk fiber extract. *Research in Microbiology* 153: 647–652.

Fabros JR D, Kankeaw U, Ruansit W et al. viral potential of cinnamon essential oil and its derived benzimidazole against porcine reproductive and respiratory syndrome virus. *Journal of Agricultural Research and Extension* 35: 21–31.

Fani M, Teimoori A & Ghafari S. 2020. Comparison of the COVID-2019 (SARS-CoV-2) pathogenesis with SARS-CoV and MERS-CoV infections. *Future Virology* 15: 317–323.

Ferreira JC, Fadl S & Rabeh WM. 2022. Key dimer interface residues impact the catalytic activity of 3CLpro, the main protease of SARS-CoV-2. *Journal of Biological Chemistry* 298.

Ferreira JC, Fadl S, Villanueva AJ & Rabeh WM. 2021. Catalytic dyad residues His41 and Cys145 impact the catalytic activity and overall conformational fold of the main SARS-CoV-2 protease 3-chymotrypsin-like protease. *Frontiers in Chemistry* 9: 692168.

Ferreira LG, Dos Santos RN, Oliva G & Andricopulo Ad. 2015. Molecular docking and structure-based drug design strategies. *Molecules* 20: 13384–13421.

Geng H-W, Zhang X-L, Wang G-C et al. 2011. Antiviral dicaffeoyl derivatives from *Elephantopus scaber*. *Journal of Asian Natural Products Research* 13: 665–669.

Govender N, Zulkifli NS, Hisham Nfb, AB Ghani NS & Mohamed-Hussein Z-A 2022. Pea eggplant (Solanum torvum Swartz) is a source of plant food polyphenols with SARS-CoV inhibiting potential. *Peer Journal* 10: e14168.

Gschwend Da, Good Ac & Kuntz Id. 1996. Molecular docking towards drug discovery. Journal of Molecular Recognition: *An Interdisciplinary Journal* 9: 175–186.

Guo T, Fan Y, Chen M et al. 2020. Cardiovascular implications of fatal outcomes of patients with coronavirus disease 2019 (COVID-19). *JAMA Cardiology* 5: 811–818.

Gupta Y, Kumar S, Zak SE et al. 2021. Antiviral evaluation of hydroxyethylamine analogs: Inhibitors of SARS-CoV-2 main protease (3CLpro), a virtual screening and simulation approach. *Bioorganic & Medicinal Chemistry* 47: 116393.

Hamidi JA, Ismaili N, Ahmadi F & Lajisi NH. 1996. Antiviral and cytotoxic activities of some plants used in Malaysian indigenous medicine. *Pertanika Journal of Tropical. Agricultural Science* 19: 129–136.

Harazem R, EL Rahman SA & El-Kenawy A. 2019. Evaluation of Antiviral Activity of Allium Cepa and Allium Sativum Extracts Against Newcastle Disease Virus. *Alexandria Journal for Veterinary Sciences* 61.

Hayashi K, Kamiya M & Hayashi T. 1995. Virucidal effects of the steam distillate from Houttuynia cordata and its components on HSV-1, influenza virus, and HIV. *Planta Medica* 61: 237–241.

Hazarika Z & Jha AN. 2020. A comparative evaluation of docking programs using influenza endonuclease as target protein. 2020 International Conference on Computational Performance Evaluation (ComPE), IEEE 321–326.

Hussain K, Hashmi Fk, Latif A, Ismail Z & Sadikun A. 2012. A review of the literature and latest advances in research of *Piper sarmento*sum. *Pharmaceutical Biology* 50: 1045–1052.

Hussain S, Rukhsar A, Iqbal M et al. 2024. Phytochemical Profile, Nutritional and Medicinal Value of Nigella sativa. *Biocatalysis and Agricultural Biotechnology* 103324.

Hussein G, Miyashiro H, Nakamura N et al. 2000. Inhibitory effects of Sudanese medicinal plant extracts on hepatitis C virus (HCV) protease. *Phytotherapy Research: An International Journal Devoted to Pharmacological and Toxicological Evaluation of Natural Product Derivatives* 14: 510–516.

Iberahim R, Yaacob WA & Ibrahim N. 2015. Phytochemistry, cytotoxicity and antiviral activity of *Eleusine indica* (sambau). AIP Conference Proceedings 2015. *AIP Publishing* LLC, 030013.

Ibrahim Mm, Azmi MN, Alhawarri MB, Kamal Nnsnm & Abumahmoud H. 2024. Synthesis, characterization and bioactivity of new pyridine-2 (H)-one, nicotinonitrile, and furo [2, 3-b] pyridine derivatives. *Molecular Diversity* 1–19.

Ichsyani M, Ridhanya A, Risanti M et al. 2017.Antiviral effects of *Curcuma longa* L. against dengue virus in vitro and in vivo. IOP Conference Series: Earth and Environmental Science, 2017. IOP Publishing, 012005.

Ikram A, Khalid W, Saeed F, Arshad MS, Afzaal M & Arshad Mu. 2023. Senna: As immunity boosting

herb against Covid-19 and several other diseases. *Journal of Herbal Medicine* 37: 100626.

Jassim SA & Naji MA. 2010. In vitro evaluation of the antiviral *activity of an extract of date palm* (*Phoenix dactylifera* L.) pits on a Pseudomonas phage. *Evidence-Based Complementary and Alternative Medicine* 7.

Jendele L, Krivak R, Skoda P, Novotny M & Hoksza D. 2019. PrankWeb: a web server for ligand binding site prediction and visualization. *Nucleic Acids Research* 47: W345–W349.

Jiang H, LI W, Zhou X, Zhang J & LI J. 2024. Crystal structures of coronaviral main proteases in complex with the non-covalent inhibitor X77. *International Journal of Biological Macromolecules* 276: 133706.

Jin Z, Du X, Xu Y et al. 2020. Structure of Mpro from SARS-CoV-2 and discovery of its inhibitors. *Nature* 582: 289–293.

Joffry SM, Yob N, Rofiee M et al. 2012. *Melastoma malabathricum* (L.) Smith ethnomedicinal uses, chemical constituents, and pharmacological properties: A review. *Evidence-Based Complementary and Alternative Medicine.*

Kalinke U, Barouch DH, Rizzi R et al. 2022. Clinical development and approval of COVID-19 vaccines. *Expert Review of Vaccines* 21: 609–619.

Kaur T, Madgulkar A, Bhalekar M & Asgaonkar K. 2019. Molecular docking in formulation and development. *Current Drug Discovery Technologies* 16: 30–39.

Kesheh MM, Hosseini P, Soltani S & Zandi M. 2022. An overview on the seven pathogenic human coronaviruses. *Reviews in Medical Virology* 32: e2282.

Keyaerts E, Vijgen L, Pannecouque C et al. 2007. Plant lectins are potent inhibitors of coronaviruses by interfering with two targets in the viral replication cycle. *Antiviral Research* 75: 179–187.

Khalil H, Ibrahim NA, Ahmed Aaa et al. 2017. Evaluation of the antimicrobial activities of Cymbopogon schoenanthus. *African Journal of Microbiology Research* 11: 653–659.

Konwar M & Sarma D. 2021. Advances in developing small molecule SARS 3CLpro inhibitors as potential remedy for corona virus infection. *Tetrahedron* 77: 131761.

Kumar D, Sharma C, Singh B & Singh D. 2015. Pharmacognostical, phytochemical and pharmacological profile of natural remedy *Lagenaria siceraria* (Mol.) Standly: A review. *Journal of Pharmaceutical Research International* 340–352.

Kumar S, Malhotra R & Kumar D. 2010. Euphorbia hirta: Its chemistry, traditional and medicinal uses, and pharmacological activities. *Pharmacognosy Reviews* 4: 58.

Kuo Pc, Hwang TL, Lin YT, Kuo Yc & Leu YL. 2011. Chemical constituents from *Lobelia chinensis* and their anti-virus and anti-inflammatory bioactivities. *Archives of Pharmacoligal Research* 34: 715.

Lans C & Van Asseldonk T. 2020. Dr. Duke's phytochemical and ethnobotanical databases, a cornerstone in the validation of ethnoveterinary medicinal plants, as demonstrated by data on pets in British Columbia. *Medicinal and Aromatic Plants of North America* 219–246.

Larue L, Kenzhebayeva B, Al-Thiabat MG et al. 2022. tLyp–1: A peptide suitable to target NRP–1 receptor. *Bioorganic Chemistry* 106200.

Larue L, Kenzhebayeva B, Al-Thiabat MG et al. 2023. tLyp–1: A peptide suitable to target NRP–1 receptor. *Bioorganic Chemistry* 130: 106200.

Li Cw, Chao Tl, Lai CL et al. 2024. Systematic Studies on the Anti-SARS-CoV-2 Mechanisms of Tea Polyphenol-Related Natural Products. *ACS Omega.*

Li Cx, Noreen S, Zhang LX et al. 2022. A critical analysis of SARS-CoV-2 (COVID-19) complexities, emerging variants, and therapeutic interventions and vaccination strategies. *Biomedicine & Pharmacotherapy* 146: 112550.

Liu H, Iketani S, Zask A et al. 2022. Development of optimized drug-like small molecule inhibitors of the SARS-CoV-2 3CL protease for treatment of COVID-19. *Nature communications* 13: 1891.

Long B, Brady Wj, Koyfman A & Gottlieb M. 2020. Cardiovascular complications in COVID-19. *The American Journal Of Emergency Medicine* 38: 1504–1507.

Lowe H, Steele B, Bryant J et al. 2021. Antiviral activity of Jamaican medicinal plants and isolated bioactive compounds. *Molecules* 26: 607.

Luo J, Wei W, Waldispühl J & Moitessier N. 2019. Challenges and current status of computational methods for docking small molecules to nucleic acids. *European Journal Of Medicinal Chemistry* 168: 414–425.

Mahmood MS, Mártinez JL, Aslam A et al. 2016. Antiviral effects of green tea (*Camellia sinensis*) against pathogenic viruses in human and animals (a mini-review). *African Journal of Traditional, Complementary and Alternative Medicines* 13: 176–184.

Mahrokhian SH, Tostanoski LH, Vidal SJ & Barouch DH. 2024. COVID-19 vaccines: Immune correlates and clinical outcomes. H*uman Vaccines & Immunotherapeutics* 20: 2324549.

Marrazza G, Ramalingam M, Jaisankar A et al. 2024. Advancements and emerging technologies in biosensors for rapid and accurate virus detection. *TRAC Trends in Analytical Chemistry* 117609.

Monti M, Milanetti E, Frans MT et al. 2024. Two Receptor Binding Strategy of SARS-CoV-2 Is Mediated by Both the N-Terminal and Receptor-Binding Spike Domain. *The Journal of Physical Chemistry B* 128: 451–464.

Moshawih S, Goh HP, Kifli N et al. 2023. Identification and optimization of TDP1 inhibitors from anthraquinone and chalcone derivatives: consensus scoring virtual screening and molecular simulations. *Journal of Biomolecular Structure and Dynamics* 1–25.

Mostafa A, Kandeil A, Shehata M et al. 2020. Middle east respiratory syndrome coronavirus (mers-cov): State of the science. Microorganisms 8: 991.

Mouhajir F, Hudson J, Rejdali M & Towers G. 2001. Multiple antiviral activities of endemic medicinal plants used by Berber peoples of Morocco. *Pharmaceutical Biology* 39: 364–374.

Musarra-Pizzo M, Pennisi R, Ben-Amor I et al. 2021. Antiviral activity exerted by natural products against human viruses. *Viruses* 13: 828.

Nikomtat J, Pinnak P, Lapmak K Et Al. 2017. Inhibition of Herpes Simplex Virus Type 2 In Vitro by Durian (*Durio zibethinus* Murray) Seed Coat Crude Extracts. *Applied Mechanics and Materials Trans Tech Publ* 60–64.

Norgan AP, Coffman Pk, Kocher J-PA, Katzmann DJ & Sosa CP. 2011. Multilevel parallelization of AutoDock 4.2. *J. Cheminform.* 3: 1–9.

Novak J & Potemkin VA. 2022. A new glimpse on the active site of SARS-CoV-2 3CLpro, coupled with drug repurposing study. *Molecular Diversity* 1–15.

Ojueromi OO, Oboh G & Ademosun AO. 2022. Black seed (*Nigella sativa*): a favourable alternative therapy for inflammatory and immune system disorders. *Inflammopharmacology* 30: 1623–1643.

Olsson MH, Søndergaard CR, Rostkowski M & Jensen J H. 2011. PROPKA3: consistent treatment of internal and surface residues in empirical p K a predictions. *J. Chem. Theory Comput.* 7: 525–537.

Omigie I & Agoreyo F. 2014. Effects of watermelon (*Citrullus lanatus*) seed on blood glucose and electrolyte parameters in diabetic wistar rats. *Journal of Applied Sciences and Environmental Management* 18: 231–233.

Ono L, Wollinger W, Rocco I M et al. 2003. In vitro and in vivo antiviral properties of sulfated galactomannans against yellow fever virus (BeH111 strain) and dengue 1 virus (Hawaii strain). *Antiviral Research* 60: 201–208.

Pai Sm, Othman AA, Rusch L et al. 2021. Science and evidence-based review and approval of covid-19 vaccines: A statement of support for the us fda. *The Journal of Clinical Pharmacology* 61: 277–279.

Parhira S, Yang Zf, Zhu Gy et al. 2014. In vitro anti-influenza virus activities of a new lignan glycoside from the latex of *Calotropis gigantea. PloS One* 9: e104544.

Paules CI, Marston HD & Fauci AS. 2020. Coronavirus infections—more than just the common cold. *JAMA* 323: 707–708.

Peddu V, Shean RC, Xie H et al. 2020. Metagenomic analysis reveals clinical SARS-CoV-2 infection and bacterial or viral superinfection and colonization. *Clinical Chemistry* 66: 966–972.

Peng C, LV X, Zhang Z, Lin J & LI D. 2024. The Recognition Pathway of the SARS-CoV-2 Spike Receptor-Binding Domain to Human Angiotensin-Converting Enzyme 2. *Molecules* 29: 1875.

Prashanth C, Geetha K, Wilson B & Banu S. 2024. Traditional uses, bioactive composition and pharmacological activities of Lens culinaris. *South African Journal of Botany* 168: 542–561.

Qiao J, LI Ys, Zeng R et al.2021. SARS-CoV-2 Mpro inhibitors with antiviral activity in a transgenic mouse model. *Science* 371: 1374–1378.

Ratnoglik SL, Aoki C, Sudarmono P et al. 2014. Antiviral activity of extracts from Morinda citrifolia leaves and chlorophyll catabolites, pheophorbide a and pyropheophorbide a, against hepatitis C virus. *Microbiology and Immunology* 58: 188–194.

Riaz F, Hameed A & Asghar MJ. 2024. Grain nutritional and antioxidant profiling of diverse lentil (Lens culinaris Medikus) genetic resources revealed genotypes with high nutritional value. *Frontiers in Nutrition* 11: 1344986.

Ritz T, Salsman ML, Young DA et al. 2021. Boosting nitric oxide in stress and respiratory infection: potential relevance for asthma and COVID-19. *Brain, Behavior, & Immunity-Health* 14: 100255.

Romeilah RM, Fayed SA & Mahmoud GI. 2010. Chemical compositions, antiviral and antioxidant activities of seven essential oils. *Journal of Applied Sciences Research* 6: 50–62.

Roy S, Sarkar T & Chakraborty R. 2022. Vegetable seeds: A new perspective in future food development. *Journal of Food Processing and Preservation* 46: e17118.

Saeed M, Khan Ms, Amir K et al. 2022. *Lagenaria siceraria* fruit: A review of its phytochemistry, pharmacology, and promising traditional uses. *Frontiers in Nutrition* 9: 927361.

San Chang J, Wang KC, Yeh CF et al. 2013. Fresh ginger (*Zingiber officinale*) has anti-viral activity against human respiratory syncytial virus in human respiratory tract cell lines. *Journal of Ethnopharmacology* 145: 146–151.

Schwartz J, Capistrano Kj, Gluck J et al. 2024. SARS-CoV-2, periodontal pathogens, and host factors: The trinity of oral post-acute sequelae of COVID-19. *Reviews in Medical Virology* 3: e2543.

Sealy RE & Hurwitz JL. 2021. Cross-reactive immune responses toward the common cold human coronaviruses and severe acute respiratory syndrome coronavirus 2 (SARS-CoV-2): Mini-review and a murine study. *Microorganisms* 9: 1643.

Shalayel MH, Al-Mazaideh GM, Aladaileh SH et al. 2020. Vitamin D is a potential inhibitor of COVID-19: In silico molecular docking to the binding site of SARS-CoV-2 endoribonuclease Nsp15. *Pakistan Journal of Pharmaceutical Sciences* 33.

Shang J, Han N, Chen Z et al. 2021. Compositional diversity and evolutionary pattern of coronavirus accessory proteins. *Briefings in Bioinformatics* 22: 1267–1278.

Singam T, Marsi NB, Abdul Rashid Ahb et al. 2020. A review on characteristics and potential applications of henna leaves (*Lawsonia inermis*). *Journal of Computational and Theoretical Nanoscience* 17: 603–612.

Sinha A, Meena A, Panda P et al. 2012. Phytochemical, pharmacological and therapeutic potential of *Hordeum vulgare* Linn.-a review. *Asian Journal of Researchi in Chemistry* 5: 1303–1308.

Srivastava K & Singh MK. 2021. Drug repurposing in COVID-19: A review with past, present and future. *Metabolism Open* 12: 100121.

Sriwilaijaroen N, Fukumoto S, Kumagai K et al. 2012. Antiviral effects of *Psidium guajava* Linn. (guava) tea on the growth of clinical isolated H1N1 viruses: Its role in viral hemagglutination and neuraminidase inhibition. *Antiviral Research* 94: 139–146.

Stoddard SV, Stoddard SD, Oelkers BK et al. 2020. Optimization rules for SARS-CoV-2 Mpro antivirals: Ensemble docking and exploration of the coronavirus protease active site. *Viruses* 12: 942.

Tahir MM, Ibrahim N & Yaacob WA. 2014. Cytotoxicity and antiviral activities of *Asplenium nidus*, *Phaleria macrocarpa* and *Eleusine indica.* AIP Conference Proceedings 2014. *American Institute of Physics* 549–

552.

Tang LI, Ling AP, Koh RY et al. 2012. Screening of anti-dengue activity in methanolic extracts of medicinal plants. *BMC complementary and Alternative Medicine* 12: 3.

Tripathi MK, Shrivastava SK, Karthikeyan S, Sinha D & Nath A. 2021. Application of machine learning and molecular modeling in drug discovery and cheminformatics. *Advanced AI Techniques and Applications in Bioinformatics*. CRC Press.

Ulasli M, Gurses SA, Bayraktar R et al. 2014. The effects of Nigella sativa (Ns), Anthemis hyalina (Ah) and *Citrus sinensis* (Cs) extracts on the replication of coronavirus and the expression of TRP genes family. *Molecular Biology Reports* 41: 1703–1711.

Varshney K & Mishra K. 2022. An analysis of health benefits of beetroot. International *Journal of Innovative Research in Engineering & Management* 9: 207–210.

Venu LN & Austin A. 2020. Antiviral efficacy of medicinal plants against respiratory viruses: Respiratory Syncytial Virus (RSV) and Coronavirus (CoV)/ COVID 19. *J Pharmacol* 9l: 281–290.

Wang W, Li Q, Wu J et al. 2021. Lentil lectin derived from *Lens culinaris* exhibit broad antiviral activities against SARS-CoV-2 variants. *Emerging Microbes & Infections* 10: 1519–1529.

Weng YL, Naik SR, Dingelstad N et al. 2021. Molecular dynamics and in silico mutagenesis on the reversible inhibitor-bound SARS-CoV-2 main protease complexes reveal the role of lateral pocket in enhancing the ligand affinity. *Scientific Reports* 11: 7429.

Wiart C, Kumar K, Yusof M et al. 2005. Antiviral properties of ent-labdene diterpenes of *Andrographis paniculata* nees, inhibitors of herpes simplex virus type 1. *Phytotherapy Research: An International Journal Devoted to Pharmacological and Toxicological Evaluation of Natural Product Derivatives* 19: 1069–1070.

Williams CJ, Headd JJ, Moriarty NW et al. 2018. MolProbity: More and better reference data for improved all-atom structure validation. *Protein Science* 27: 293–315.

Woster PM. 2009. Foreword: American Chemical Society Division of Medicinal Chemistry. Celebrating 100 Years of Excellence. *Journal of Medicinal Chemistry* 52: 7333–7338.

Wu F, Zhou Y, LI L et al. 2020. Computational approaches in preclinical studies on drug discovery and development. *Frontiers in Chemistry* 8: 726.

Yan JK, Zhu J, Liu Y et al. 2023. Recent advances in research on Allium plants: Functional ingredients, physiological activities, and applications in agricultural and food sciences. *Critical Reviews in Food Science and Nutrition* 63: 8107–8135.

Yan S & WU G. 2021. Potential 3-chymotrypsin-like cysteine protease cleavage sites in the coronavirus polyproteins pp1a and pp1ab and their possible relevance to COVID-19 vaccine and drug development. *The FASEB Journal* 35.

Yang YL, Wang B, LI W et al. 2024. Functional dissection of the spike glycoprotein S1 subunit and identification of cellular cofactors for regulation of swine acute diarrhea syndrome coronavirus entry. *Journal of Virology* 98: e0013924.

Yunos NM, Al-Thiabat MG & Sallehudin NJ. 2024. Quassinoids from Eurycoma longifolia as Potential Dihydrofolate Reductase Inhibitors: A Computational Study. *Current Pharmaceutical Biotechnology*.

Yunos NM, Wahab HA, Al-Thiabat MG, Sallehudin NJ & Jauri MH. 2023. In Vitro and In Silico Analysis of the Anticancer Effects of Eurycomanone and Eurycomalactone from *Eurycoma longifolia*. *Plants* 12: 2827.

Zakaryan H, Arabyan E, OO A & Zandi K. 2017. Flavonoids: promising natural compounds against viral infections. *Archives of Virology* 162: 2539–2551.

Zanetti-Polzi L, Smith MD, Chipot C et al. 2021. Tuning proton transfer thermodynamics in SARS-CoV-2 main protease: Implications for catalysis and inhibitor design. *The Journal Of Physical Chemistry Letters* 12: 4195–4202.

Zearah SA. 2024. Assessment of the antioxidant potential of anthocyanin-rich Extract of eggplant (*Solanum melongena* L.) and evaluation of its antimicrobial activity. *Tropical Journal of Natural Product Research* 8: 6558–6562.

Zhang B, LI H, YU K & Jin Z. 2022. Molecular docking-based computational platform for high-throughput virtual screening. *CCF Transactions on High Performance Computing* 1–12.

Zhu Z, Lian X, SU X et al. 2020. From SARS and MERS to COVID-19: a brief summary and comparison of severe acute respiratory infections caused by three highly pathogenic human coronaviruses. *Respiratory Research* 21: 1–14.